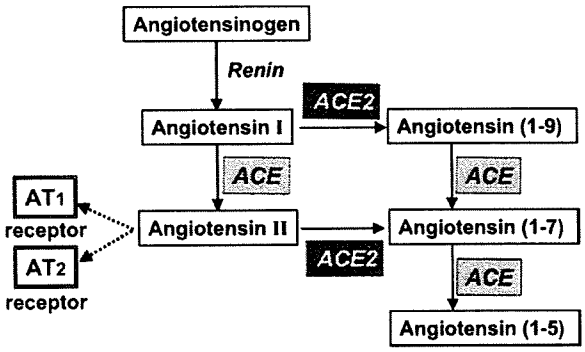

Figure 1 Schematic illustration of the renin-angiotensin system. Abbreviations: ACE, angiotensin-converting enzyme; AT_1, angiotensin II type-1 receptor; AT_2, angiotensin II type-2 receptor.

Methods

Patients

Patients were examined in the Department of Neurology at Kyushu University Hospital and the Departments of Anesthesiology and Resuscitology at Ehime University Hospital, Japan from 2003 to 2007. Informed consent was obtained from each individual and the study protocol was approved by the ethics committees of both hospitals. We obtained CSF samples from 20 patients with MS and 17 controls that had neither neurological diseases nor any other diseases that might affect the angiotensin II levels in the CSF. The controls underwent lumbar puncture during spinal anesthesia for operations for either urological or gynecological disorders. The control group was comprised of 7 females and 10 males. The average age at examination was 49.4 ± 14.3 (mean ± SD) years. All patients with MS fulfilled the McDonald criteria [6]. Patients with MS included 16 females and 4 males. The average age at examination was 40.4 ± 15.7 years and the disease duration was 36.1 ± 40.9 months. All patients were suffering from relapsing–remitting MS, and CSF was taken at relapse (within 30 days of the initiation of relapse) before introduction of any immunological treatment, except for two patients on long-term interferon β-1b. Six patients had opticospinal MS (OSMS), whereas the rest had conventional MS (CMS) [7]. The patient's average Kurtzke's Expanded Disability Status Scale (EDSS) [8] score was 4.3 ± 2.7. None of the patients had hypertension, hypotension, or a metabolic disorder, and none took antihypertensive drugs. CSF samples were immediately centrifuged at 800 rpm at 4 °C for 5 min. The liquid phase of CSF excluding sedimented cells was stored at −80 °C until required for the cytokine assay. The average CSF cell counts and protein amounts were 8.2 ± 19.5/μL and 39.9 ± 39.3 mg/dL, respectively, in the MS group.

Measurement of angiotensin II, ACE, and ACE2 concentrations in the CSF

Angiotensin II, ACE, and ACE2 concentrations in the CSF were measured by established enzyme-linked immunosorbent assay (ELISA) systems for angiotensin II (SPI-bio, Montigny-le-Bretonneux, France), ACE (R&D Systems, Minneapolis, Minnesota, USA), and ACE2 (AdipoGen Inc., Seoul, Korea). According to the manufacturer's data, the precision, recovery, and linearity of these assays are as follows: for the human ACE ELISA, the intra-assay coefficients of variation (CVs) are 3.4–4.0%, inter-assay CVs are 4.9–7.7%, the recovery range is 91–106% and linearity is around 105% of expected; for the human ACE2 ELISA, the intra-assay CVs are 5.3–9.9%, inter-assay CVs are 5.4–10.8%, the recovery range is 81–113%, and linearity is around 100% of expected.

Statistical analysis

Statistical analyses of angiotensin II, ACE, and ACE2 levels were performed using the Mann–Whitney *U*-test. Correlation between angiotensin II, ACE, and ACE2 levels and various clinical parameters was analyzed by the Spearman test. A value of $P < 0.05$ was considered to be statistically significant.

Results

Angiotensin II levels in the CSF were 3.8 ± 1.58 pg/mL in the MS group (3.67 ± 1.24 pg/mL in patients with CMS and 4.08 ± 2.23 pg/mL in patients with OSMS), and 5.93 ± 2.18 pg/mL in the control group. The difference between the MS group and the control group ($P = 0.005$) was statistically significant. ACE levels in the CSF were 48.42 ± 4.84 pg/mL in the MS group (49.04 ± 5.36 pg/mL in patients with CMS and 46.96 ± 3.30 pg/mL in patients with OSMS) and 44.71 ± 3.9 pg/mL in the control group, and the difference between the MS group and the control ($P = 0.010$) was statistically significant. ACE2 levels in the CSF were 2.56 ± 0.26 pg/mL in the MS group (2.61 ± 0.27 pg/mL in patients with CMS and 2.43 ± 0.17 pg/mL in patients with OSMS) and 2.78 ± 0.24 pg/mL in the control group, and the difference between the MS group and the control ($P = 0.017$) was statistically significant (Figure 2). There were no significant differences between patients with CMS and OSMS in any of the above-mentioned parameters. No significant correlation was found

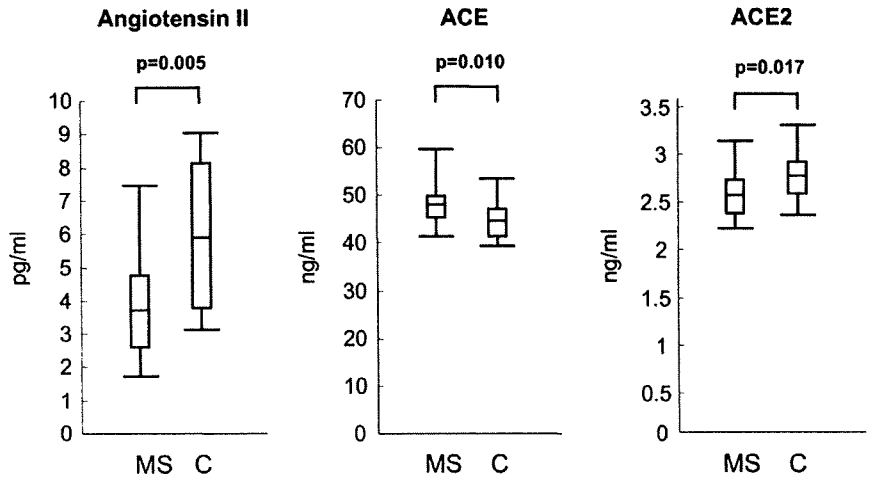

Figure 2 Comparison of angiotensin II, angiotensin-converting enzyme (ACE), and ACE2 levels in the cerebrospinal fluid (CSF) of patients with multiple sclerosis (MS) and control individuals (C).

between ACE/ACE2 levels and clinical parameters, such as age at onset and examination, sex, disease duration, EDSS, CSF cell counts, and protein amounts. There was no significant correlation between angiotensin II levels and either ACE or ACE2 levels in patients with MS or controls.

Discussion

In the present study, we reported decreased levels of ACE2 in CSF from patients with MS for the first time. We also confirmed our previous finding that angiotensin II levels are reduced in MS CSF [3], and confirmed another previous finding that ACE levels are elevated in MS CSF [5]. These results further support the notion that the RAS is altered intrathecally in MS.

In ACE2-null mice, serum angiotensin II levels dramatically increased after the infusion of angiotensin II compared with the levels in wild-type littermates, indicating that ACE2 metabolizes angiotensin II *in vivo* [9]. However, the biology of ACE2 in the central nervous system (CNS) is completely unknown. Some studies speculate that ACE and ACE2 expression may be regulated in parallel or synergistically while such a concept of parallel regulation has been questioned by others.

Wosik, *et al.* [10] recently reported that levels of perivascular astrocytes immunopositive for angiotensinogen were reduced in MS lesions, and that this reduction correlated with reduced expression of the tight junction protein occludin. Angiotensin II is thus considered to upregulate expression of occludin and strengthen the blood–brain barrier (BBB). Therefore, decreased production of angiotensin II is assumed to contribute to BBB dysfunction in patients with MS. Increased levels of ACE, which produces angiotensin II, and decreased levels of ACE2, which degrades angiotensin II, may represent the body's effort to partly compensate for the reduced amount of angiotensinogen in patients with MS. Further studies to measure the levels of angiotensinogen and angiotensin-(1–7) in the CSF are necessary to uncover abnormalities in the RAS in the CNS of patients with MS.

Acknowledgements

This work was supported in part by a grant from the Research Committees of Neuroimmunological Diseases of the Ministry of Health, Labor, and Welfare of Japan, the Ministry of Education, Science, Sports, and Culture of Japan, the Suzuken Memorial Foundation, and the Takeda Science Foundation.

References

1. Mogi, M, Li, JM, Iwanami, J, *et al.* Angiotensin II type-2 receptor stimulation prevents neural damage by transcriptional activation of methyl methanesulfonate sensitive 2. *Hypertension* 2006; **48**: 141–148.
2. Li, JM, Mogi, M, Tsukuda, K, *et al.* Angiotensin II-induced neural differentiation via angiotensin II type 2 (AT2) receptor-MMS2 cascade involving interaction between AT2 receptor-interacting protein and Src homology 2 domain-containing protein-tyrosine phosphatase 1. *Mol Endocrinol* 2007; **21**: 499–511.
3. Kawajiri, M, Mogi, M, Osoegawa, M, *et al.* Reduction of angiotensin II in the cerebrospinal fluid of patients with multiple sclerosis. *Multiple Sclerosis* 2008; **14**: 557–560.

4. Ferrario, CM. Angiotensin-converting enzyme 2 and angiotensin-(1-7): an evolving story in cardiovascular regulation. *Hypertension* 2006; **47**: 515–521.
5. Constantinescu, CS, Goodman, DB, Grossman, RI, Mannon, LJ, Cohen, JA. Serum angiotensin-converting enzyme in multiple sclerosis. *Arch Neurol* 1997; **54**: 1012–1015.
6. McDonald, WI, Compston, A, Edan, G, *et al.* Recommended diagnostic criteria for multiple sclerosis: guidelines from the International Panel on the diagnosis of multiple sclerosis. *Ann Neurol* 2001; **50**: 121–127.
7. Kira, J, Kanai, T, Nishimura, Y, *et al.* Western versus Asian types of multiple sclerosis: immunogenetically and clinically distinct disorders. *Ann Neurol* 1996; **40**: 569–574.
8. Kurtzke, JF. Rating neurologic impairment in multiple sclerosis: an expanded disability status scale (EDSS). *Neurology* 1983; **33**: 1444–1452.
9. Gurley, SB, Allred, A, Le, TH, *et al.* Altered blood pressure responses and normal cardiac phenotype in ACE2-null mice. *J Clin Invest* 2006; **116**: 2218–2225.
10. Wosik, K, Cayrol, R, Dodelet-Devillers, A, *et al.* Angiotensin II controls occludin function and is required for blood brain barrier maintenance: relevance to multiple sclerosis. *J Neurosci* 2007; **27**: 9032–9042.

RESEARCH PAPER *Multiple Sclerosis* 2009; **15**: 304–310

Hypercomplementemia at relapse in patients with anti-aquaporin-4 antibody

H Doi, T Matsushita, N Isobe, T Matsuoka, M Minohara, H Ochi and JI Kira

Objective Because Asian patients with opticospinal multiple sclerosis (OSMS) frequently have anti-aquaporin-4 (AQP4) antibody, complement-mediated disruption of astrocyte foot processes is proposed but not yet proven. We aimed to clarify whether complement consumption occurs at relapse in anti-AQP4 antibody-positive patients.

Methods We analyzed serum CH50, C3, C4, and C-reactive protein (CRP) levels and their relation to clinical phases in 118 MS patients with or without anti-AQP4 antibody. Serum CH50 levels were higher in 24 patients with anti-AQP4 antibody than in 39 OSMS and 54 conventional form of MS (CMS) patients without anti-AQP4 antibody at relapse ($P^{corr} < 0.05$) but not in remission. The frequency of hypercomplementemia at relapse was also higher in anti-AQP4 antibody-positive patients than in anti-AQP4 antibody-negative CMS patients (70.4% vs 29.0%, $P^{corr} < 0.05$). C3 and C4 levels did not differ significantly among the three groups at relapse. In patients with anti-AQP4 antibody, the coexistence of hypercomplementemia and high CRP values was more common at relapse than in the remission phase (36.0% vs 10.5%, $P < 0.05$). In patients with extensive central nervous system lesions, hypercomplementemia was significantly more common in anti-AQP4 antibody-positive patients than anti-AQP4 antibody-negative ones (88.9% vs 16.7%, $P < 0.01$). We consider that hypercomplementemia in anti-AQP4 antibody-positive patients may reflect a systemic inflammatory reaction at relapse. *Multiple Sclerosis* 2009; **15**: 304–310. http://msj.sagepub.com

Key words: anti-aquaporin-4 antibody; hypercomplementemia; multiple sclerosis; neuromyelitis optica

Introduction

Multiple sclerosis (MS) is an inflammatory demyelinating disease of the central nervous system (CNS) that is generally considered to be mediated by myelin-autoreactive T cells [1]. By contrast, neuromyelitis optica (NMO) is characterized by severe and selective involvement of the optic nerves and spinal cord, the latter of which frequently shows longitudinally extensive spinal cord lesions (LESCLs) extending over three or more vertebral segments [2,3]. Recently, a specific IgG against NMO, designated NMO-IgG, was described [4]; its relevant antigen was reported to be aquaporin-4 (AQP4) [5]. Because of the high specificity of NMO-IgG and anti-AQP4 antibody, NMO has been claimed to be a distinct disease entity with a fundamentally different causal mechanism from MS [3].

In Asians, the selective and severe involvement of the optic nerves and spinal cord is characteristic [6], and there are two distinct subtypes of MS: the opticospinal form of MS (OSMS), which has similar features to the relapsing-remitting form of NMO in Western populations [2,7–9], and the conventional form of MS (CMS), which is associated with disseminated lesions in the CNS, including the cerebrum, cerebellum, and brainstem [7], similar to classical MS in Western populations [6,7,10,11]. In a selected series of Japanese patients with OSMS, Nakashima, *et al.* [12] reported an NMO-IgG positivity rate of approximately 60%, and OSMS has now been suggested to be NMO [3].

Additionally, a highly significant correlation between anti-AQP4 antibody titer and spinal cord lesion length was reported [13], and selective loss of AQP4 from the acute lesions in autopsied OSMS

Department of Neurology, Neurological Institute, Graduate School of Medical Sciences, Kyushu University, Fukuoka, Japan
Correspondence to: Jun-ichi Kira, MD, PhD, Professor and Chairman, Department of Neurology, Neurological Institute, Graduate School of Medical Sciences, Kyushu University, 3-1-1 Maidashi, Higashi-ku, Fukuoka 812-8582, Japan. Email: kira@neuro.med.kyushu-u.ac.jp
Received 25 June 2008; revised 16 September 2008; accepted 24 September 2008

 10.1177/1352458508099139

spinal cord specimens has been described [14,15]. Anti-AQP4 antibody was recently shown to induce AQP4 down-modulation *in vitro* using AQP4-transfected cells [16]. Therefore, it is hypothesized that anti-AQP4 antibody is a causative agent for both NMO and OSMS, and that demyelination is secondarily produced following damage to the astrocyte foot process, where AQP4 is localized [14,15,17]. As anti-AQP4 antibodies belong mainly to the IgG1 subclass, complement-mediated injury is postulated [16] but not yet proven *in vivo*. In other autoimmune diseases, such as systemic lupus erythematosus (SLE) and Sjögren's syndrome, serum complement levels decrease at relapse because of consumption and are predictive of prognosis [18–21]. Therefore, in the present study, we aimed to clarify the relationships of serum complement levels, such as those of CH50, C3, and C4, with anti-AQP4 antibody status, disease phase, the extent of the CNS lesions on magnetic resonance imaging (MRI), including LESCLs and the extensive white matter lesions occasionally seen in this condition [22,23], and systemic inflammatory reaction as measured by C-reactive protein (CRP) levels in MS patients with or without anti-AQP4 antibody.

Methods

Patients

We retrospectively investigated serum complement (C3, C4, and CH50) and CRP levels measured between January 2003 and March 2008 and their relations to clinical phases in patients with clinically definite MS by Poser's criteria [24] at Kyushu University Hospital. We classified patients with MS into three groups: anti-AQP4 antibody-positive patients, anti-AQP4 antibody-negative OSMS patients, and anti-AQP4 antibody-negative CMS patients. The clinical classification of OSMS and CMS was according to Kira, *et al.* [7]. Among 118 patients enrolled, 25 were positive for anti-AQP4 antibody, 39 were anti-AQP4 antibody-negative OSMS patients, and 54 were anti-AQP4 antibody-negative CMS patients (Table 1). The disability status of the patients was scored by one of the authors (JK), according to the Expanded Disability Status Scale (EDSS) [25]. Severe optic neuritis was defined as grade 5 or more than 5 on Kurtzke's Visual Functional Scale (FS) [25]. Acute transverse myelopathy (ATM) was defined according to Fukazawa, *et al.* [26]. Levels of anti-AQP4 antibody were measured by an indirect immunofluorescence method using green fluorescent protein (GFP)-AQP4 fusion protein-transfected human embryonic kidney cells (HEK-293), as previously described [23].

Measurement of complement and CRP

C3 and C4 levels were determined by turbidimetric immunoassay, and CH50 activity was determined by liposome immunoassay. CRP levels were measured by latex photometric immunoassay. Normal ranges were 71–135 mg/dL for C3, 11–34 mg/dL for C4, 20–50 U/mL for CH50, and <0.10 mg/dL for CRP. We defined hypercomplementemia as CH50 activity higher than 50 U/mL, and values higher than 60 U/mL were all recorded as 60 U/mL because of the limitation of the assay system. Eighty serum samples were measured during the relapsing phase and 256 samples were measured in the remission phase (27 and 64 samples from anti-AQP4 antibody-negative patients, 22 and 98 samples from anti-AQP4 antibody-negative OSMS patients, and

Table 1 Demographic features of multiple sclerosis subgroups

	Total ($n = 118$)	AQP4-Ab (+) MS ($n = 25$)	AQP4-Ab (–) OSMS ($n = 39$)	AQP4-Ab (–) CMS ($n = 54$)
No. of males/females	27/91	1/24*	7/32	19/35*
Age at examination (years old)	44.8 ± 13.3	50.1 ± 13.8*	47.9 ± 12.8**	40.1 ± 12.0*,**
Disease duration (years)	12.8 ± 9.2	13.8 ± 8.2	13.4 ± 9.7	11.9 ± 9.2
EDSS score at last visit	3.7 ± 2.5	4.6 ± 2.5*	4.0 ± 2.8	3.0 ± 2.2
Severe visual impairment (≥FS 5)	49/114 (43.0%)	17/24 (70.8%)*	17/38 (44.7%)	15/52 (28.8%)*
Acute transverse myelopathy	38/117 (32.5%)	12/24 (50.0%)*	20/39 (51.3%)**	6/54 (11.1%)*,**
LESCL during entire course	48/118 (40.7%)	18/25 (64.0%)*	18/39 (46.2%)	12/54 (22.2%)*
Anti-nuclear antibody	21/118 (17.8%)	10/25 (40.0%)*	6/39 (15.4%)	6/54 (11.1%)*
Anti-SS-A/SS-B antibody	17/118 (14.4%)	6/25 (24.0%)	5/39 (12.8%)	6/54 (11.1%)
Sjögren's syndrome/SLE	5/118 (4.2%)	3/25 (12.0%)	2/39 (5.1%)	0/54 (0.0%)

AQP4-Ab (+) MS, anti-aquaporin-4 antibody-positive multiple sclerosis; AQP4-Ab (–) OSMS, anti-aquaporin-4 antibody-negative opticospinal form of multiple sclerosis; AQP4-Ab (–) CMS, anti-aquaporin-4 antibody-negative conventional form of multiple sclerosis; EDSS, Expanded Disability Status Scale; FS, Visual Functional Scale; LESCL, longitudinally extensive spinal cord lesion; SLE, Systemic lupus erythematosus.

*Statistically significant between AQP4-Ab (+) MS and AQP4-Ab (–) CMS ($P^{corr} < 0.05$).

**Statistically significant between AQP4-Ab (–) OSMS and AQP4-Ab (–) CMS ($P^{corr} < 0.05$).

31 and 94 samples from anti-AQP4 antibody-negative CMS patients).

Magnetic resonance imaging

All MRI studies were performed using 1.5-T units, Magnetom Vision and Symphony (Siemens Medical Systems, Erlangen, Germany), as previously described [27]. LESCLs were defined as lesions extending over three or more vertebral segments on sagittal MRI [2,3], and extensive white matter lesions were defined as lesions more than 30 mm across on axial MRI [27]. We obtained 18 MRI samples from anti-AQP4 antibody-positive patients, 17 from anti-AQP4 antibody-negative OSMS patients, and 25 from anti-AQP4 antibody-negative CMS patients in the relapsing phase (within 30 days of the initiation of the relapse) at the time when the complement levels in these patients were measured.

Statistical analyses

The chi-square test and Fisher's exact test were used to compare categorical values. For comparison to continuous values, we used the nonparametric Kruskal–Wallis test for non-normally distributed variables. When statistical significance was found, the Mann–Whitney *U*-test was used to determine the statistical significance of the differences between them. Uncorrelated *P* values were corrected by multiplying them by the number of comparisons (Bonferroni-Dunn's correction) to calculate corrected *P* values. The correlation between CH50 and CRP levels was analyzed by Spearman's rank correlation test. *P* values <0.05 were considered to represent statistical significance.

Results

Demographic features

In 25 patients with anti-AQP4 antibody, the clinical phenotype was OSMS in 19 and CMS in six. Among them, 19 patients (16 with OSMS and three with CMS) fulfilled the revised diagnostic criteria for NMO [3]. Anti-AQP4 antibody-positive patients had a significantly higher age at onset, higher EDSS scores, and higher frequencies of severe visual impairment, ATM, LESCLs during the entire clinical course, and anti-nuclear antibody than anti-AQP4 antibody-negative CMS patients ($P^{corr} < 0.05$ in all), whereas disease duration was not significantly different among the three groups (Table 1). Anti-AQP4 antibody-negative OSMS patients also showed a higher age at onset and higher frequency of ATM than anti-AQP4 antibody-negative CMS patients ($P^{corr} < 0.05$ in all).

Complement levels

Serum CH50 levels in the relapsing phase were significantly higher in patients with anti-AQP4 antibody (52.3 ± 7.2 U/mL) than in anti-AQP4 antibody-negative OSMS (47.2 ± 6.9 U/mL, $P^{corr} < 0.05$) and CMS patients (44.0 ± 10.1 U/mL, $P^{corr} < 0.005$) (Figure 1A). The frequency of hypercomplementemia (CH50 > 50 U/mL) in the relapsing phase was significantly higher in patients with anti-AQP4 antibody than in anti-AQP4 antibody-negative CMS patients (19/27, 70.4% vs 9/31, 29.0%, $P^{corr} < 0.05$), whereas it was not different between anti-AQP4 antibody-negative OSMS (8/22, 36.4%) and CMS patients. In the remission phase, the frequency of hypercomplementemia was not significantly different among the three groups (23/64, 35.9% in anti-AQP4 antibody-positive patients; 28/98, 28.6% in anti-AQP4 antibody-negative OSMS patients; and 25/94, 26.6% in anti-AQP4 antibody-negative CMS patients). The serum levels of C3 and C4 were not significantly different among the three groups, regardless of clinical phase, except for higher levels of C3 in anti-AQP4 antibody-positive patients than anti-AQP4 antibody-negative CMS patients in the remission phase (107.9 ± 19.2 vs 98.9 ± 19.7 mg/dL, $P^{corr} < 0.05$) (Figure 1B, C). The frequencies of patients with high C3 or C4 levels were not significantly different among the three groups, irrespective of clinical phase, except for the frequency of patients with high C4 levels in the remission phase, which was greater among anti-AQP4 antibody-negative OSMS patients than among anti-AQP4 antibody-negative CMS patients (17/109, 15.6% vs 5/100, 5.0%, $P^{corr} < 0.05$).

CRP levels

Serum CRP levels at relapse were not different significantly among the three groups (Figure 2A). The frequency of high CRP levels (>0.1) at relapse was significantly higher in anti-AQP4 antibody-positive patients (13/28, 46.4%) than anti-AQP4 antibody-negative CMS patients (5/35, 14.3%) ($P^{corr} < 0.05$), whereas anti-AQP4 antibody-negative OSMS patients (9/24, 37.5%) showed a similar high frequency to anti-AQP4 antibody-positive patients. This trend persisted even in the remission phase, yet the difference was not significant.

Correlation between serum CH50 and CRP levels

The frequency of patients who had both hypercomplementemia and high CRP values was significantly higher among anti-AQP4 antibody-positive patients

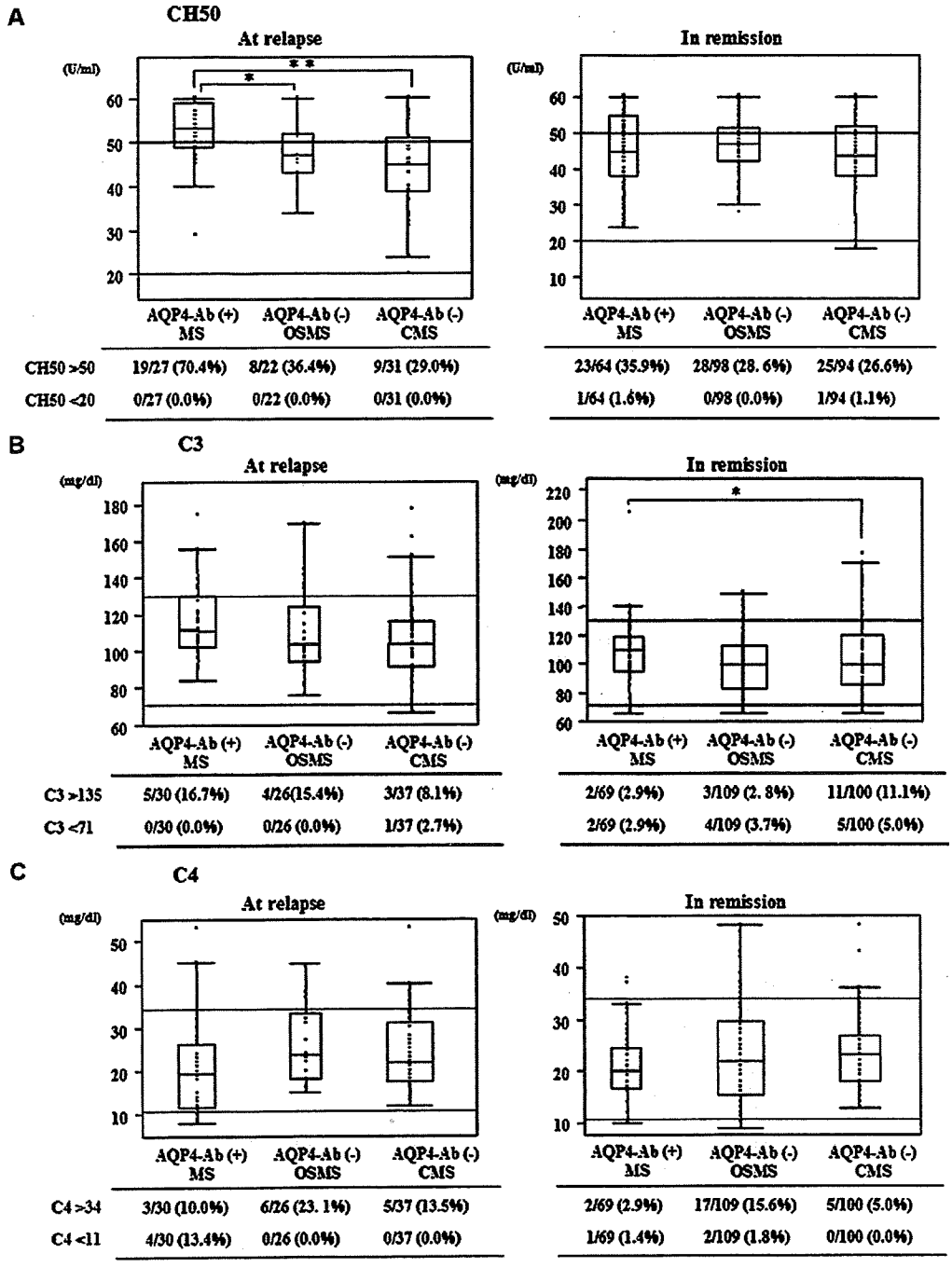

Figure 1 (A) CH50, (B) C3, and (C) C4 values in anti-AQP4 antibody-positive MS patients, anti-AQP4 antibody-negative OSMS patients, and anti-AQP4 antibody-negative CMS patients. $*p^{corr} < 0.05$, $**p^{corr} < 0.005$.

than among anti-AQP4 antibody-negative CMS patients in the relapse phase (9/25, 36.0% vs 3/30, 10.0%, $P^{corr} < 0.05$), whereas it was not significantly different among the three groups in the remission phase (Figure 2B). Anti-AQP4 antibody-negative OSMS patients again showed an intermediate frequency between the two in the relapse phase (5/21, 23.8%). Among patients with anti-AQP4 antibody, the frequency of those with both hypercomplementemia and high CRP values was significantly higher at

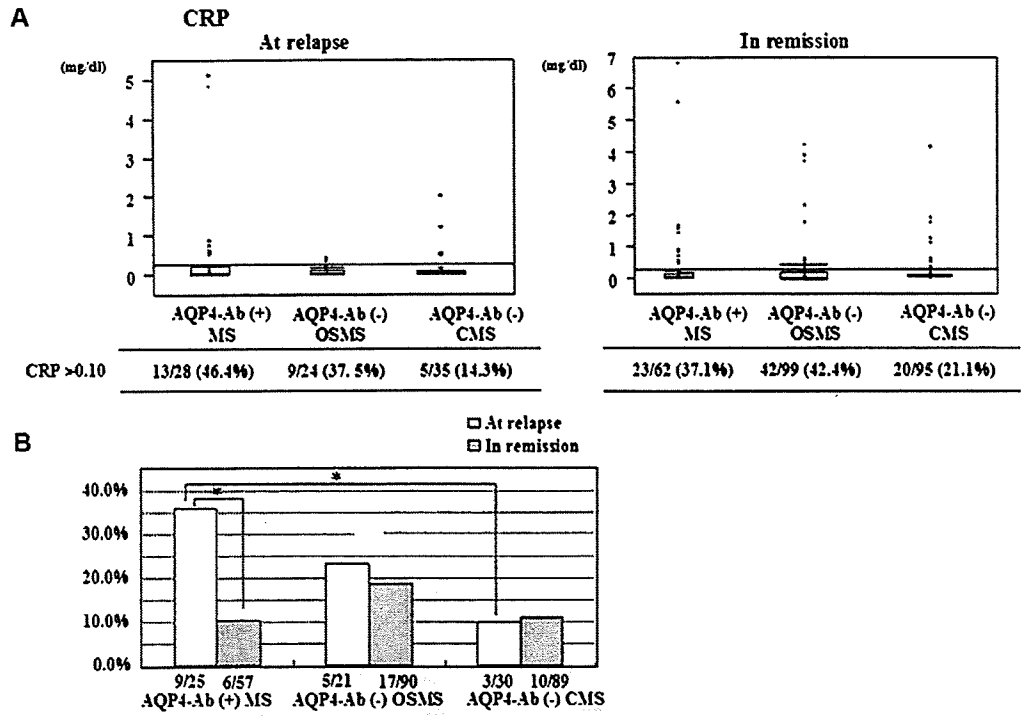

Figure 2 (A) CRP values and (B) the frequencies of patients with both hypercomplementemia and high CRP values among anti-AQP4 antibody-positive MS patients, anti-AQP4 antibody-negative OSMS patients, and anti-AQP4 antibody-negative CMS patients. $*P^{corr} < 0.05$.

relapse than in the remission phase (36.0% vs 10.5%, $P < 0.05$). There was no significant correlation between CH50 and CRP levels in anti-AQP4 antibody-positive patients.

Correlation between hypercomplementemia and extensive CNS lesions at relapse

Among patients with hypercomplementemia, anti-AQP4 antibody-positive patients had a significantly higher frequency of extensive CNS lesions than anti-AQP4 antibody-negative patients (66.7% vs 16.7%, $P < 0.05$) (Figure 3A). Moreover, among patients with extensive CNS lesions, the frequency of hypercomplementemia was significantly greater in patients with anti-AQP4 antibody than in those without the antibody (88.9% vs 16.7%, $P < 0.01$) (Figure 3B).

Discussion

In the present study, we show for the first time the occurrence of hypercomplementemia in anti-AQP4 antibody-positive patients at the time of relapse, but not in the remission phase, and that this occurrence is associated with systemic inflammatory reactions as shown by high CRP values. We also found that hypercomplementemia coincided with the emergence of extensive CNS lesions, such as LESCLs and extensive white matter lesions, in anti-AQP4 antibody-positive patients.

Complement is part of the innate immune system and underlies not only one of the effector mechanisms of antibody-mediated immunity but also constitutes one of a host's acute-phase reactions [28]. Although anti-AQP4 antibody is specifically observed in patients with relapsing NMO or OSMS, its emergence is frequently associated with systemic autoimmune diseases, such as Sjögren's syndrome and SLE [23]. In these conditions, hypocomplementemia is especially related to acute exacerbation [18,19], reflecting complement activation and consumption *in vivo*. Because the anti-AQP4 antibodies so far examined are mainly of the IgG1 subclass, with high complement fixing activity, they are claimed to disrupt astrocyte foot processes by fixing and activating complements once specifically bound to the AQP4 molecule on the cell surface [15,16]. However, evidence of complement consumption was not obtained at relapse in the present study; rather, most patients had heightened CH50 activity, which is in sharp contrast to humoral immunity-mediated systemic

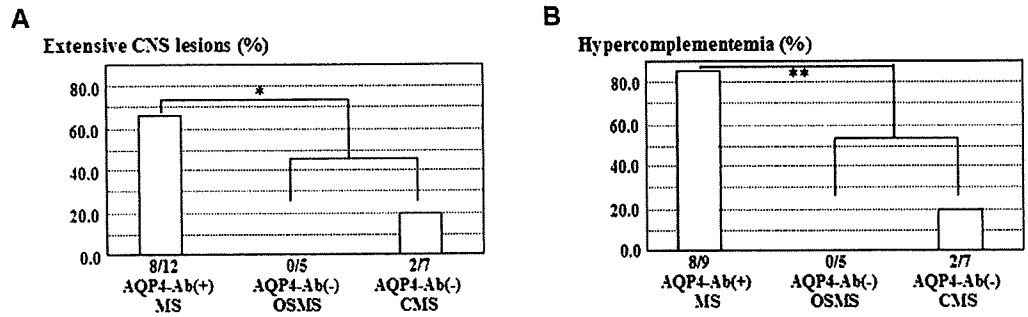

Figure 3 (A) Frequency of extensive CNS lesions in patients with hypercomplementemia at relapse. (B) Frequency of hypercomplementemia in patients with extensive CNS lesions at relapse. $*P < 0.05$, $**P < 0.005$.

autoimmune diseases, such as Sjögren's syndrome and SLE. Thus, most relapses in anti-AQP4 antibody-positive patients are supposed to be induced in a distinct way from those in systemic autoimmune diseases mediated by complement-fixing autoantibodies, except for some relapses (13.4%) when a decrease in the level of C4 was observed.

Hypercomplementemia has been reported to occur in association with infection, malignant tumor, and vasculitis [28,29]. Cases with concurrent infection were excluded as much as possible in the present study, and coexistence of malignancy was unconceivable in the majority of our patients with more than 10 years of disease duration. A significant increase in the number of anti-AQP4 antibody-positive patients showing both hypercomplementemia and high CRP values at relapse suggests that hypercomplementemia is a reflection of a systemic acute inflammatory reaction, such as vasculitis. The mild increase in CRP values without overt infection in about half of anti-AQP4 antibody-positive patients also indicates the existence of systemic inflammation, which may contribute to the development of relapse, but its cause remains unknown. An association between hypercomplementemia and the occurrence of the extensive CNS lesions may indicate a role of such systemic inflammatory reactions in lesion formation in this condition.

It is interesting to note that even among anti-AQP4 antibody-negative OSMS patients, about 40% of the patients showed a mild increase in the level of CRP. This suggests that systemic inflammatory reactions tend to commonly underlie relapses in OSMS or NMO cases, regardless of the presence or absence of anti-AQP4 antibody. We recently reported that CSF cytokine and chemokines are markedly upregulated in OSMS and NMO patients, irrespective of anti-AQP4 antibody status [30]. Initiation of inflammation at relapse may occur independently from the existence of anti-AQP4 antibody in these conditions. The high frequency of raised CRP values, even in the remission phase in anti-AQP4 antibody-positive patients and anti-AQP4 antibody-negative OSMS patients, suggests that mild but persistent systemic inflammation may be a key component of these conditions.

Acknowledgements

This work was supported in part by grants from the Research Committees of Neuroimmunological Diseases, the Ministry of Health, Labour and Welfare, Japan and from the Ministry of Education, Culture, Sports, Science and Technology, Japan.

References

1. McFarland, HF, Martin, R. Multiple sclerosis: a complicated picture of autoimmunity. *Nature Imunol* 2007; **8**: 913–919.
2. Wingerchuk, DM, Hogancamp, WF, O'Brien, PC, Weinshenker, BG. The clinical course of neuromyelitis optica (Devic's syndrome). *Neurology* 1999; **53**: 1107–1114.
3. Wingerchuk, DM, Lennon, VA, Pittock, SJ, Lucchinetti, CF, Weinshenker, BG. Revised diagnostic criteria for neuromyelitis optica. *Neurology* 2006; **66**: 1485–1489.
4. Lennon, VA, Wingerchuk, DM, Kryzer, TJ, *et al.* A serum autoantibody marker of neuromyelitis optica: distinction from multiple sclerosis. *Lancet* 2004; **364**: 2106–2112.
5. Lennon, VA, Kryzer, TJ, Pittock, SJ, Verkman, AS, Hinson, SR. IgG marker of optic-spinal multiple sclerosis binds to the aquaporin-4 water channel. *J Exp Med* 2005; **202**: 473–477.
6. Kira, J. Multiple sclerosis in the Japanese population. *Lancet Neurol* 2003; **2**: 117–127.
7. Kira, J, Kanai, T, Nishimura, Y, *et al.* Western versus Asian types of multiple sclerosis: immunogenetically and clinically distinct disorders. *Ann Neurol* 1996; **40**: 569–574.
8. Cree, BA, Goodin, DS, Hauser, SL. Neuromyelitis optica. *Semin Neurol* 2002; **22**: 105–122.
9. Lucchinetti, CF, Mandler, RN, McGavern, D, *et al.* A role for humoral mechanisms in the pathogenesis of Devic's neuromyelitis optica. *Brain* 2002; **125**: 1450–1461.
10. Yamasaki, K, Horiuchi, I, Minohara, M, *et al.* HLA-DPB1*0501-associated opticospinal multiple sclerosis:

clinical, neuroimaging and immunogenetic studies. *Brain* 1999; **122**: 1689–1696.
11. Ishizu, T, Osoegawa, M, Mei, FJ, *et al.* Intrathecal activation of the IL-17/IL-8 axis in opticospinal multiple sclerosis. *Brain* 2005; **128**: 988–1002.
12. Nakashima, I, Fujihara, K, Miyazawa, I, *et al.* Clinical and MRI features of Japanese patients with multiple sclerosis positive for NMO-IgG. *J Neurol Neurosurg Psychatry* 2006; **77**: 1073–1075.
13. Takahashi, T, Fujihara, K, Nakashima, I, *et al.* Anti-aquaporin-4 antibody is involved in the pathogenesis of NMO: a study on antibody titre. *Brain* 2007; **130**: 1235–1243.
14. Roemer, SF, Parisi, JE, Lennon, VA, *et al.* Pattern-specific loss of aquaporin-4 immunoreactivity distinguishes neuromyelitis optica from multiple sclerosis. *Brain* 2007; **130**: 1194–1205.
15. Misu, T, Fujihara, K, Kakita, A, *et al.* Loss of aquaporin 4 in lesions of neuromyelitis optica: distinction from multiple sclerosis. *Brain* 2007; **130**: 1224–1234.
16. Hinson, SR, Pittock, SJ, Lucchinetti, CF, *et al.* Pathogenic potential of IgG binding to water channel extracellular domain in neuromyelitis optica. *Neurology* 2007; **69**: 2221–2231.
17. Jacob, A, Matiello, M, Wingerchuk, DM, Lucchinetti, CF, Pittock, SJ, Weinshenker, BG. Neuromyelitis optica: changing concepts. *J Neuroimmunol* 2007; **187**: 126–138.
18. Ramos-Casals, M, Campoamor, MT, Chamorro, A, *et al.* Hypocomplementaemia in systemic lupus erythematosus and primary antiphspholipid syndrome: prevalence and clinical significance in 667 patients. *Lupus* 2004; **13**: 773–783.
19. Ramos-Casals, M, Brito-Zerón, P, Yagüe, J, *et al.* Hypocomplementaemia as an immunological marker of morbidity and mortality in patients with primary Sjögren's syndrome. *Rheumatology* 2005; **44**: 89–94.
20. Alexander, EL, Provost, TT, Sanders, ME, Frank, MM, Joiner, KA. Serum complement activation in central nervous system disease in Sjögren's syndrome. *Am J Med* 1988; **85**: 513–518.
21. Brito-Zerón, P, Ramos-Casals, M, Bove, A, Sentis, J, Font, J. Predicting adverse outcomes in primary Sjögren's syndrome: identification of prognostic factors. *Rheumatology* 2007; **46**: 1359–1362.
22. Pittock, SJ, Lennon, VA, Krecke, K, Wingerchuk, DM, Lucchinetti, CF, Weinshenker, BG. Brain abnormalities in neuromyelitis optica. *Arch Neurol* 2006; **63**: 390–396.
23. Matsuoka, T, Matsushita, T, Kawano, Y, *et al.* Heterogeneity of aquaporin-4 autoimmunity and spinal cord lesions in multiple sclerosis in Japanese. *Brain* 2007; **130**: 1206–1223.
24. Poser, CM, Paty, DW, Scheinberg, L, *et al.* New diagnostic criteria for multiple sclerosis: guidelines for research protocols. *Ann Neurol* 1983; **13**: 227–231.
25. Kurtzke, JF. Rating neurologic impairment in multiple sclerosis: an expanded disability status scale (EDSS). *Neurology* 1983; **33**: 1444–1452.
26. Fukazawa, T, Hamada, T, Tashiro, K, Moriwaka, F, Yanagihara, T. Acute transverse myelopathy in multiple sclerosis. *J Neurol Sci* 1990; **100**: 217–222.
27. Matsushita, T, Matsuoka, T, Ishizu, T, *et al.* Anterior periventricular linear lesions in optic-spinal multiple sclerosis: a combined neuroimaging and neuropathological study. *Mult Scler* 2008; **14**: 343–353.
28. Walport, MJ. Complement: first of two parts. *N Eng J Med* 2001; **344**: 1058–1066.
29. Lin, CY, Hwang, B. Serial immunologic studies in patients with mucocutaneous lymph node syndrome (Kawasaki disease). *Ann Allergy* 1987; **59**: 291–297.
30. Tanaka, M, Tanaka, M, Matsushita, T, *et al.* Distinct CSF cytokine/chemokine profiles in atopic myelitis and other causes of myelitis. *Neurology* 2008; **71**: 974–981.

NeuroImage 51 (2010) 412–420

Contents lists available at ScienceDirect

NeuroImage

journal homepage: www.elsevier.com/locate/ynimg

Oscillatory gamma synchronization binds the primary and secondary somatosensory areas in humans

Koichi Hagiwara [a,b,1], Tsuyoshi Okamoto [c,1], Hiroshi Shigeto [a,b,*], Katsuya Ogata [b], Yuko Somehara [b], Takuya Matsushita [a], Jun-ichi Kira [a], Shozo Tobimatsu [b]

[a] Department of Neurology, Neurological Institute, Graduate School of Medical Sciences, Kyushu University, Fukuoka, Japan
[b] Department of Clinical Neurophysiology, Neurological Institute, Graduate School of Medical Sciences, Kyushu University, Fukuoka, Japan
[c] Digital Organ, Digital Medicine Initiative, Kyushu University, Fukuoka, Japan

ARTICLE INFO

Article history:
Received 1 September 2009
Revised 14 December 2009
Accepted 2 February 2010
Available online 10 February 2010

Keywords:
Primary somatosensory cortex (SI)
Secondary somatosensory cortex (SII)
Magnetoencephalography (MEG)
Functional connectivity
Induced gamma
Phase-locking value (PLV)

ABSTRACT

Induced gamma activity has a key role in the temporal binding of distributed cortico-cortical processing. To elucidate the neural synchronization in the early-stage somatosensory processing, we studied the functional connectivity between the primary and secondary somatosensory cortices (SI and SII) in healthy subjects using magnetoencephalography (MEG) with excellent spatiotemporal resolution. First, somatosensory-evoked magnetic fields were recorded to determine the locations of each cortical activity. Then we analyzed the phase-locking values (PLVs) of the induced gamma activity to assess neural synchrony within the somatosensory cortical network. We also assessed PLVs in patients with multiple sclerosis (MS) to validate our PLV analysis in evaluating the inter-areal functional connectivity, which can often be impaired in MS. The PLVs of the induced gamma activity were calculated for each pair of unaveraged MEG signals that represented the activities of the contralateral SI and bilateral SII areas. Analysis of PLVs between the SI and SII areas showed significantly increased PLVs for gamma-band activities, starting at an early post-stimulus stage in normal controls, whereas this increase in PLVs was apparently diminished in MS. The PLV analysis provided evidence for early-latency, gamma-band neuronal synchronization between the SI and SII areas in normal controls. Our study first demonstrates the gamma-band synchrony in the early-stage human somatosensory processing.

Introduction

In the somatosensory system, the primary and secondary somatosensory cortices (SI and SII) comprise the early stage of the hierarchical organization. Numerous neurophysiological studies have examined the functional differences between the two cortical areas in humans. Electrophysiological studies of evoked responses have often reported differences in activation timing between SI and SII (Pons et al., 1987; Mauguière et al., 1997; Inui et al., 2004), with the SI response occurring earlier than the SII responses. There are also studies with direct intracortical recording in epilepsy patients, which proved that SI and SII were activated in a sequential manner (Frot and Mauguière, 1999; Balzamo et al., 2004). The typical characteristics of SII include sensitivity towards higher order functions, such as sensorimotor integrations, attention, unitary body image, and integration of nociceptive and non-nociceptive information (for a review, see Lin and Forss, 2002). Anatomically, it has been shown that the neurons in SII have larger and more complex receptive fields than those in SI (for a review, see Iwamura, 1998). Therefore, SII is often considered to be a hierarchically higher cortical area than SI.

Less is known about the functional connectivity between SI and SII in humans. Apart from the activation sequence of the cortical areas, few studies have evaluated functional connectivity between SI and SII in humans. Recently, it has become evident that neuronal synchronization plays an important role in distributed cortico-cortical processing: induced gamma activity could be related to the temporal binding of spatially distributed information processing in the mammalian brain (Tallon-Baudry and Bertrand, 1999; Engel and Singer, 2001; Buzsáki and Draguhn, 2004; Knight, 2007). To date, however, whether the temporal binding mechanism with the gamma-band activity relates to the somatosensory processing between SI and SII has not been demonstrated. To clarify this issue, we applied magnetoencephalography (MEG) to evaluate neural synchrony in the gamma-band during the median nerve stimulation in healthy subjects. We analyzed phase-locking values (PLVs) of induced gamma activity between the somatosensory cortices. To validate our PLV analysis in evaluating functional connectivity between the distributed cortical areas, we also assessed PLVs in patients with

* Corresponding author. Department of Clinical Neurophysiology, Neurological Institute, Graduate School of Medical Sciences, Kyushu University, 3-1-1 Maidashi, Higashi-ku, Fukuoka 812-8582, Japan. Fax: +81 92 642 5352.
E-mail address: shigetou@neuro.med.kyushu-u.ac.jp (H. Shigeto).
[1] These authors contributed equally to this work.

1053-8119/$ – see front matter © 2010 Elsevier Inc. All rights reserved.
doi:10.1016/j.neuroimage.2010.02.001

clinically definite multiple sclerosis (MS). MS is known to cause multiple disconnections between distributed regions of the brain owing to demyelination and axonal loss in the central nervous system (Calabrese and Penner, 2007; Dineen et al., 2009; He et al., 2009). Here we provide evidence for early-stage, gamma-band neuronal synchronization between SI and SII for somatosensory information processing in humans.

Methods

Subjects

Twenty-three healthy volunteers (18 women and 5 men, mean age 37.3 ± 10.6 years) and 23 patients with clinically definite MS (18 women and 5 men, mean age 38.8 ± 8.1 years) according to the revised McDonald criteria (Polman et al., 2005) participated in this study. With respect to the MS patients, the mean duration of disease was 10.0 ± 7.3 years, and the mean Kurtzke Expanded Disability Status Scale Score (Kurtzke, 1983) was 2.7 ± 2.7. The clinical courses of the patients were relapsing–remitting in 17 patients, secondary progressive in four patients, and primary progressive in two patients. All the patients showed only mild disability and were ambulatory. On the basis of clinical histories obtained during routine follow-up, clinically evident sensory symptoms were documented in the right arm in 10 patients, and in the left arm, in nine patients. Somatosensory-evoked potentials were measured in 19 patients, and either delayed central conduction time or an absent N20 response was observed in four patients in response to right median nerve stimulation and seven patients in response to left median nerve stimulation. Nineteen patients showed typical brain lesions fulfilling the Barkhof magnetic resonance imaging (MRI) criteria (Barkhof et al., 1997): nine T2 hyperintense lesions present in nineteen patients, at least one infratentorial lesion present in seventeen patients, at least one juxtacortical lesion present in seventeen patients, at least three periventricular lesions present in twenty-two patients. In most patients, their clinical manifestations were usually caused by lesions in the optic nerves, brainstem, cerebellum, and spinal cord. No patients showed cognitive decline. None of the patients had anti-aquaporin-4 antibody, as confirmed by immunofluorescence technique (Matsuoka et al., 2007). Four patients were examined during a relapse period. This study was approved by the local ethics committees of our university, and written consent was obtained from all subjects.

Stimuli

Left and right median nerves were stimulated at the wrist in a separate recording with constant current pulses of 0.2-ms duration. The stimulus intensity was adjusted above the motor threshold to produce slight contraction of the abductor pollicis brevis muscle. At this intensity, large myelinated fibers but not small ones were stimulated. The stimuli were given pseudo-randomly, and the inter-stimulus interval ranged from 2.5 to 3.5 s (mean interval: 3 s) to avoid habituation of SII responses.

Data acquisition and processing

The MEG signals were acquired using a whole-head 306-channel sensor array (Vectorview, ELEKTA Neuromag, Helsinki) that comprises 102 identical triple-sensor elements. Each sensor element consists of two orthogonal planar-type gradiometers and one magnetometer. In this study, we analyzed MEG data recorded by the 204-channel planar-type gradiometers (gradiometers reduce external artifact signals, including geomagnetic signals and other environmental artifact signals). Prior to the recording, four head position indicator (HPI) coils were attached to the scalp, and a 3D digitizer was used to measure anatomical landmarks of the head with respect to the HPI coils. During the recording, subjects lay on a bed in a magnetically shielded room with their heads positioned inside the helmet-shaped sensor array. The precise location of the head with respect to the sensor array was determined using the HPI coils. The recording bandpass filter was 0.03–1500 Hz, and the sampling rate was 5 kHz. The subjects were instructed to keep their eyes open and not to sleep; their vigilance levels were monitored by spontaneous MEG signals over the parieto-occipital areas and a video camera positioned in a shielded room. During the stimulation, we only stored raw data for off-line analysis. A spatiotemporal signal space separation (tSSS) method was applied off-line to the recorded raw data. tSSS is a software method that removes artifact signals arising from outside the sensor helmet (Taulu and Simola, 2006), and thus, theoretically, only artifact-free raw data were stored for further analysis.

Data analysis

Analysis of somatosensory-evoked magnetic fields (SEFs)

First, we analyzed conventional SEFs to determine the sensors representing activities of SI and SII. Off-line averaging of SEFs was performed using the tSSS-reconstructed raw data in the following condition: the analysis epoch was 50 ms before and 250 ms after the stimulus, and 100–120 responses were averaged for each median nerve. The averaged responses were digitally bandpass filtered in the 0.3–150 Hz range with a notch filter of 60 Hz. The prestimulus period from −50 ms to −10 ms was used as a baseline. The peak latencies and amplitudes of SEF waveforms were determined by root-mean-square (RMS) waveforms reconstructed from the two orthogonal gradiometers to better identify the sensors showing the maximal responses (Kida et al., 2006). We analyzed evoked responses generated by three sources: the SI area in the hemisphere contralateral to the median nerve stimulation (cSI) and the bilateral secondary somatosensory areas (cSII and iSII, for contralateral and ipsilateral SII areas, respectively). For responses in cSI, three deflections (i.e., N20m, P35m, and P60m) were recorded. For each of the five deflections (N20m, P35m, P60m, cSII, and iSII), we searched for the sensor with the maximum amplitude, and peak latencies were determined at the time point showing the maximal amplitude. In the somatosensory paradigm used in this study, several cortical areas other than SI and SII could be activated such as the posterior parietal cortex and the mesial cortex of the paracentral lobule (Forss et al., 1994, 1996; Mauguière et al., 1997). Here, we focused on SI and SII responses to elucidate the functional interaction of these somatosensory cortices.

Equivalent current dipoles (ECDs) that explained the most dominant sources of each deflection were calculated by a least-squares fit using approximately 30 channels around the sensor with the maximum response. For analysis of the bilateral SII responses, the ECD of the P35m deflection (if P35m was not apparent, then P60m) was subtracted from the original waveforms using the signal space projection (SSP) method to remove the magnetic fields of cSI, because the isocontour fields of cSII could be hidden by those of cSI. The ECD analysis yielded the three-dimensional locations and strengths of the ECDs in a spherical conductor model. Because MRI was performed only in four subjects from the control group, the centers of the individual head coordinate system were standardized using the center of device coordinate ($x=0$ mm, $y=0$ mm, $z=40$ mm) in both groups. Only the ECDs with goodness-of-fit values exceeding 80% were accepted for statistical analyses.

The peak latencies and amplitudes of the RMS waveforms were examined by Mann–Whitney *U*-test. The correlation between the latencies of cSI and bilateral SII responses was assessed by calculating Pearson's correlation coefficient. A Chi-square test was used to compare the numbers of evoked deflections between normal subjects and MS

patients. A probability level of 0.05 or less was considered to represent a significant difference throughout the statistical examinations.

Phase-locking analysis of gamma-band cortical activity

To evaluate the neuronal synchronization between the SI and SII areas, we calculated the PLVs of the stimulus-related gamma-band activity (Lachaux et al., 1999). First, to analyze oscillatory gamma-band activity, a continuous wavelet transform was applied to the tSSS reconstructed raw data. A temporal-frequency response is given by the temporal convolution of an MEG signal with the wavelet centering at center frequency f_0 and time t:

$$\Phi_k^m(t,f_0) = \int_{-\infty}^{\infty} s_k^m(\tau)\Psi_{f_0}{}^*(\tau - t)d\tau$$

where $s_k^m(\tau)$ represents the signal of kth trial recorded by channel m. In this transformation, we used a complex Morlet wavelet:

$$\Psi_{f_0}(\tau) = \frac{1}{\sqrt{\omega_0}} exp\left(-\frac{\tau^2}{2\sigma^2}\right) exp(i\omega_0\tau)$$

where $\omega_0 = 2\pi f_0$, $\omega_0\sigma = 7$. The wavelet analysis yielded induced gamma-band activities. Epochs for the wavelet transformation ranged from −250 to 350 ms relative to the stimulus onset. Second, we selected a sensor with maximal RMS amplitude of N20m deflection as a sensor representing cSI activity, and sensors with maximal RMS amplitudes of cSII and iSII responses were determined as sensors

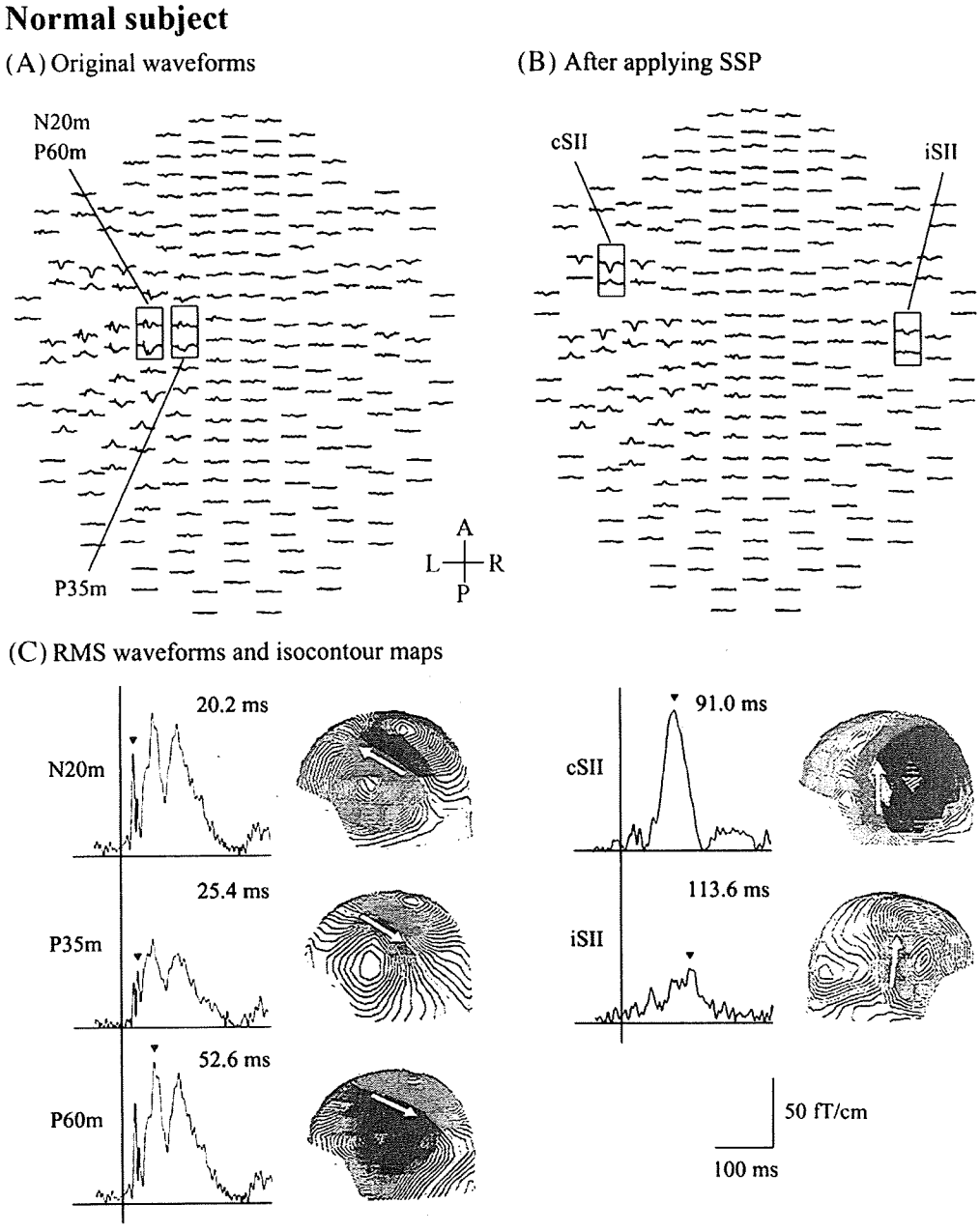

Fig. 1. Analysis of SEFs in a representative normal subject. (A) Original SEF waveforms are averaged from the tSSS reconstructed signals. (B) After subtracting the P35m response from the original waveforms by the SSP method, the sensors show only bilateral SII responses. (C) RMS waveforms at sensors with maximal peak amplitude of each deflection and corresponding field distributions (isocontour maps). The red lines indicate outgoing magnetic signals, while the blue lines ingoing magnetic signals. The arrows denote the current direction of the corresponding ECDs.

representing bilateral SII activities. PLV between two channels was calculated as follows:

$$PLV^{m,n}(t,f_0) = \left| \frac{1}{N}\sum_{k=1}^{N} \frac{\Phi_k^m(t,f_0)}{|\Phi_k^m(t,f_0)|} \Big/ \frac{\Phi_k^n(t,f_0)}{|\Phi_k^n(t,f_0)|} \right|$$

where m and n denote channels comprising the reference sensor and target sensor, respectively. PLV was calculated for each single trial, and the PLVs of 100 trials were averaged in each subject. PLVs are shown as an index ranging from 0 to 1.

Third, we examined phase-locking statistics (PLS) to determine whether the calculated PLVs were significantly correlated with the stimuli. PLS was defined by the proportion of surrogate PLVs higher than the original PLVs. The surrogate PLV represents the PLV calculated between signals of different trials:

$$PLV^{m,n}_{surrogate}(t,f_0) = \left| \frac{1}{100}\sum_{k=1}^{100} \frac{\Phi^m_{perm(k)}(t,f_0)}{|\Phi^m_{perm(k)}(t,f_0)|} \Big/ \frac{\Phi_k^n(t,f_0)}{|\Phi_k^n(t,f_0)|} \right|$$

Here, we calculated the surrogate PLVs from 200 different permutations of trials. The statistically significant PLV was defined as the presence of surrogated PLVs of less than 10 trials larger than original PLVs (that is, PLS<0.05). Furthermore, the mean PLV of the prestimulus period (−100 to 0 ms) was subtracted from the PLV of the

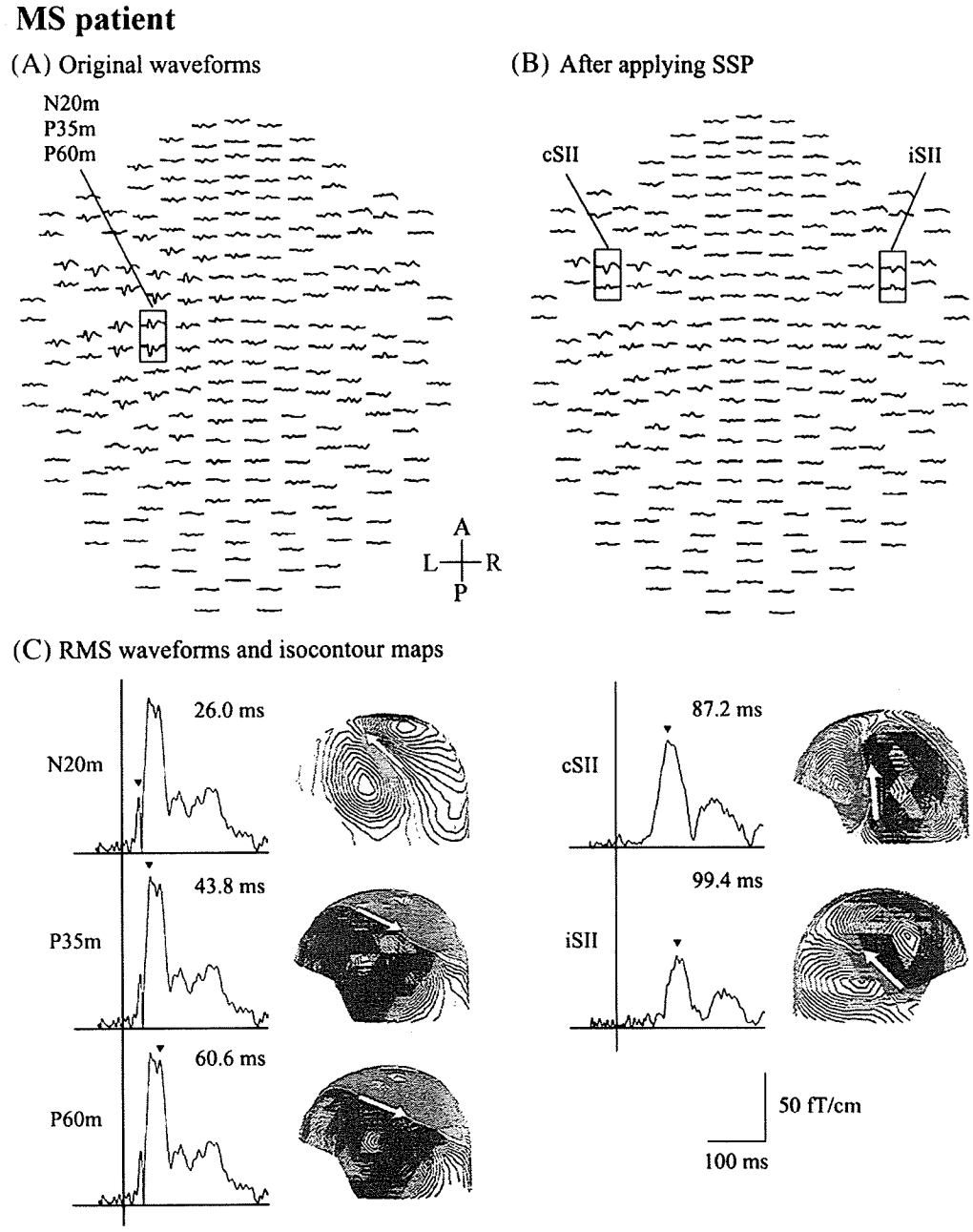

Fig. 2. Analysis of SEFs in an MS patient. The latencies of all cSI deflections (namely, N20m, P35m, and P60m) are prolonged compared with those in the normal subjects, whereas bilateral SII responses are evoked with comparable latencies. The amplitude of the N20m deflection is decreased, but other deflections, including the bilateral SII, are comparable in the amplitude to those in normal subjects.

Table 1
Latencies and amplitudes (mean ± SD) of the RMS waveforms.

	Latency (ms)			Amplitude (fT/cm)		
	Normal	MS	p value	Normal	MS	p value
N20m	21.4 ± 1.0 (n = 46)	23.5 ± 3.8 (n = 45)	0.027*	64.9 ± 30.1	52.1 ± 25.9	0.018*
P35m	32.0 ± 5.0 (n = 46)	35.6 ± 6.5 (n = 40)	0.005*	75.3 ± 48.7	74.3 ± 39.1	0.616
P60m	53.8 ± 7.6 (n = 46)	57.8 ± 8.4 (n = 46)	0.01*	90.2 ± 31.3	88.2 ± 47.4	0.281
cSII	91.2 ± 15.8 (n = 46)	87.2 ± 14.9 (n = 46)	0.153	60.8 ± 23.4	65.0 ± 33.6	0.656
iSII	104.2 ± 19.8 (n = 44)	104.1 ± 22.9 (n = 41)	0.728	41.4 ± 18.0	41.9 ± 18.6	0.778

* P<0.05: when compared with the values in normal subjects using the Mann–Whitney U-test.

post-stimulus period; thus, only event-related phase synchronization of gamma-band activities was evaluated.

For the analysis of the group average, we selected regions of interest (ROIs) as follows: the frequency range was 30–70 Hz, and the latency period was 0–200 ms. PLVs were calculated for each orthogonally oriented pair of channels to minimize crosstalk noise, and the mean PLV was calculated from the ROI in each subject. Only PLVs with larger means were accepted for the group-averaged PLV (p<0.05 by Rayleigh test).

Results

SEFs of SI and SII

In line with the results of previous studies (Kakigi, 1994; Wikström et al., 1996; Lin and Forss, 2002; Huttunen et al., 2006), we recorded five major deflections of the SEF waveforms in the cSI and bilateral SII areas. Figs. 1 and 2 show the representative SEF waveforms and isocontour maps obtained from normal subjects and MS patients. Short-latency deflections, N20m, P35m, and P60m, which corresponded to the activities of the cSI area, were identified over the contralateral centro-parietal area. Middle-latency deflections were observed over the bilateral temporo-parietal area with the deflection contralateral to the stimulation peaking earlier than the deflection ipsilateral to the stimulation: the former corresponds to the activity of cSII, while the latter corresponds to the activity of iSII. All cSI deflections were clearly identified in all normal subjects, whereas N20m and P35m deflections were not recorded in one hemisphere (p = 0.31) and six hemispheres (p<0.01), respectively, in MS patients. The cSII deflection was identified in all normal subjects as well as in all MS patients. The iSII deflection was undetectable in two hemispheres in normal subjects and in five hemispheres in MS patients (p = 0.22).

Regarding the side-to-side difference within each group, there were no significant differences in the peak latencies or in the amplitudes between the left and right median nerves. Therefore, the data for left and right median nerve stimulations were combined for the statistical analysis. Table 1 shows the latencies and amplitudes of the RMS waveforms. The mean latencies of all of the cSI deflections were significantly prolonged in MS patients (p<0.05). By contrast, there were no significant differences in the latencies of bilateral SII deflections. In both groups, cSII and iSII were recorded at around 90 and 100 ms after stimulation, respectively. The mean amplitudes of the N20m deflection were significantly smaller in MS patients (p<0.05). The amplitudes of other deflections showed no significant differences between MS and normal subjects. No significant correlation was found between the latencies for N20m and cSII in both

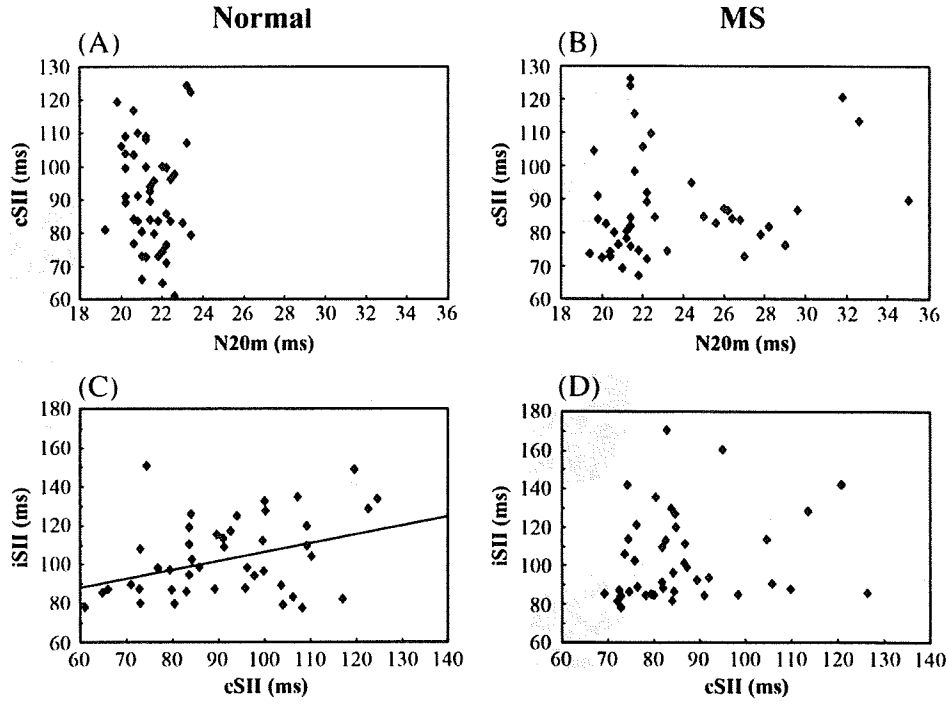

Fig. 3. A linear regression analysis of correlation between the latencies of cSI and cSII shows no significant correlation both in normal subjects (A; r = 0.09, p = 0.55) and MS patients (B; r = 0.18, p = 0.23). Correlation analysis between the latencies of cSII and iSII shows a significant correlation in normal subjects (C; r = 0.361, p = 0.016) but not in MS patients (D; r = 0.158, p = 0.323).

groups (Fig. 3A and B). There was a significant correlation between the latencies of cSII and iSII in normal subjects ($p<0.05$) (Fig. 3C), but no correlation was found in MS patients (Fig. 3D). The mean locations and strengths of the ECDs for each deflection were almost comparable with those reported previously (see Supplemental data) (Wikström et al., 1996; Wegner et al., 2000; Kida et al., 2006). Fig. 4 shows the locations of the ECDs superimposed on the MRI in representative subjects of both groups, demonstrating that the ECDs are located in the appropriate cortices (i.e., SI and SII).

PLVs between SI and SII

The temporal-frequency analysis with the continuous wavelet transformation showed the induced gamma-band activities both in the SI and SII areas (Figs. 5 and 6). They started at early post-stimulus period and continued up to 200 ms. In normal subjects, high-frequency gamma activities (50–70 Hz) were observed in cSI, and to a lesser degree in cSII. Low-frequency gamma activities (30–40 Hz) were distributed in all three areas (i.e., cSI, cSII, and iSII). Interestingly, the power of the high-frequency gamma activities (50–70 Hz) was relatively reduced in MS patients. Figs. 7 and 8 show the grand averaged PLVs in the gamma-band (30–70 Hz) for the normal subjects and MS patients. Overall, PLVs were calculated in the range of 0–0.15. In normal subjects, significantly increased PLVs between cSI and cSII were observed mostly within the time window 0–100 ms after the stimulus onset (Fig. 7A). Increased PLVs in the higher frequency gamma-band (50–70 Hz) were observed within the early period (0–50 ms) following the stimulus onset, whereas high PLVs in the lower frequency gamma-band (30–40 Hz) tended to last for a longer period, up to 100 ms. In addition, there were some weak but statistically significant PLVs of various frequency bands in the later time window 100–200 ms. On the contrary, the cSI–cSII phase synchrony was significantly decreased in MS patients, both in the high-frequency gamma-band (50–70 Hz) and the low-frequency gamma-band (30–40 Hz) (Fig. 7B). The degree of decrease in the PLVs between cSI and cSII was most prominent around 40 Hz. Regarding the phase synchrony between the cSII and iSII areas, significantly increased PLVs in the low-frequency gamma-band (30–40 Hz) were observed during the time interval 30–100 ms in normal subjects (Fig. 8A), whereas such an increase in PLVs was diminished in MS patients (Fig. 8B).

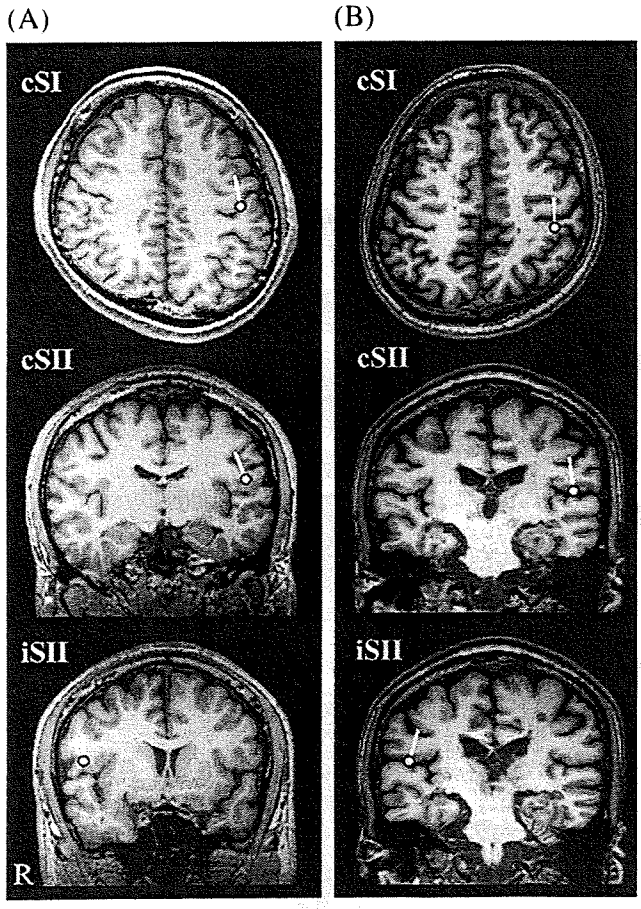

Fig. 4. ECD locations in a normal subject (A) and an MS patient (B) superimposed on MRI. For this view, cSI (N20m) and bilateral SII sources are located in the appropriate cortices in both subjects. The MS patient has scattered small hypointensities in the periventricular and juxtacortical white matter.

Discussion

Neuronal synchronization in the gamma-frequency band has received increasing attention as the salient mechanism for cortico-cortical information processing (Tallon-Baudry and Bertrand, 1999; Engel and Singer, 2001; Buzsáki and Draguhn, 2004; Knight, 2007; Womelsdorf et al., 2007). Recently, the temporal binding mechanism in various gamma-frequency bands has been well recognized in several studies of top-down and bottom-up information processing among anatomically distributed cortical areas (Tallon-Baudry et al., 1997; Engel et al., 2001; Womelsdorf et al., 2006; Buschman and Miller, 2007; Saalmann et al., 2007). However, the significance of temporal binding theory in the functional relationship between SI and SII has not yet been established. In this study, we assessed the temporal binding mechanism by PLVs of induced gamma activity, and our results provided evidence for functional interaction in the early somatosensory processing. To our knowledge, we first demonstrated that synchronized gamma-band activities in both between cSI and cSII and between cSII and iSII occurred in the early post-stimulus stage. Therefore, the oscillatory gamma synchronization binds the early-stage tactile information processing within the somatosensory cortical network.

Previous studies demonstrated that broadband oscillatory activities including the gamma-frequency bands were present and enhanced in relation to the attentive task in the early-stage somatosensory processing areas (Palva et al., 2005; Bauer et al., 2006). Until recently, no studies have examined the gamma-band phase synchronization between the SI and SII areas. Only cSI–iSII phase-locking in the alpha- and beta-frequency bands has been demonstrated in healthy subjects (Simões et al., 2003). Therefore, our study is the first to demonstrate the early-latency neural synchrony within the gamma-band between SI and SII, which may well represent the parallel mode of the early-stage tactile somatosensory processing. Although we did not perform attentive task to enhance the oscillatory gamma activity, the increase in PLVs after the stimulus onset (see Fig. 7) may be associated with ongoing cortical activities facilitating the later stages of somatosensory processing and perceptual process (Palva et al., 2005).

It is well known that SII receives direct thalamocortical projections from several nuclei of the thalamus, including the ventroposterior lateral nucleus, the ventroposterior inferior nucleus, the ventroposterior medial nucleus, the central lateral nucleus, and the posterior nucleus (Friedman and Murray, 1986; Krubitzer and Kaas, 1992; Stevens et al., 1993). In a study that applied a cortical cooling procedure in marmoset monkeys (Zhang et al., 1996, 2001), evoked responses and responsiveness of individual neurons in SII were rarely abolished by inactivation of SI, and the study claimed that SI and SII occupied a hierarchically equivalent position in the somatosensory system. In humans, simultaneous activation of SI and SII was suggested by an MEG study (Karhu and Tesche, 1999), which demonstrated very early evoked responses of SII; the initial activity

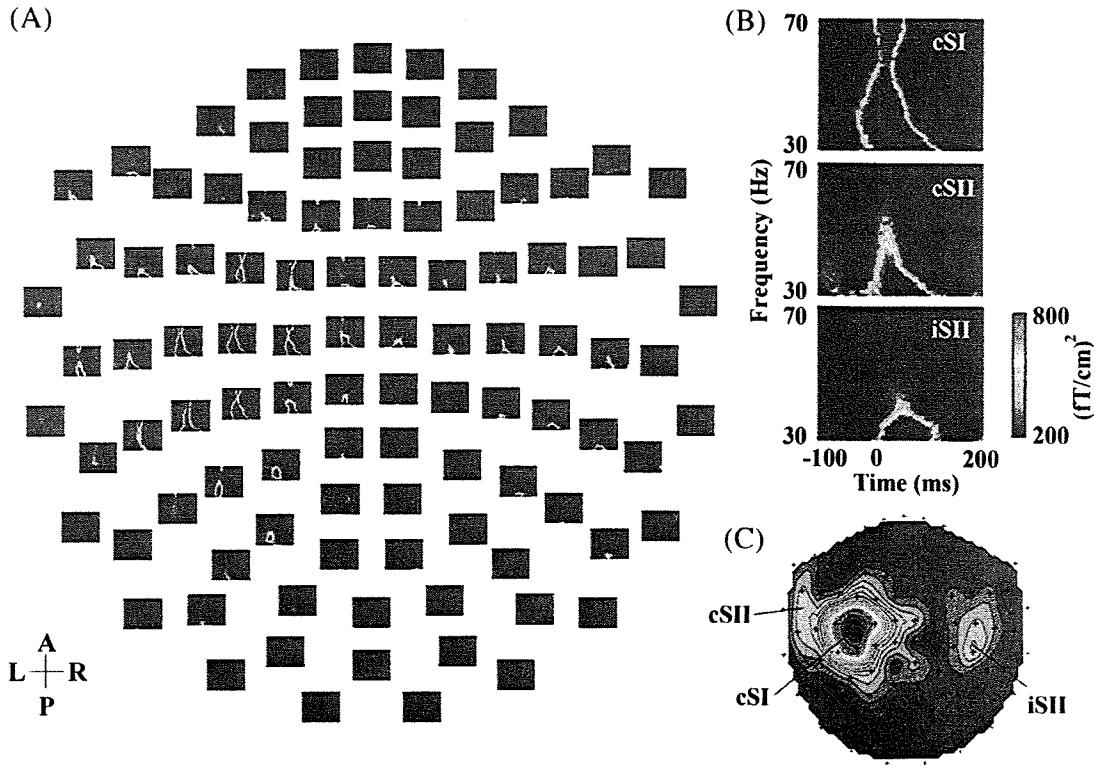

Fig. 5. (A) Temporal-frequency analysis for all gradiometer sensors in a representative normal subject. (B) Induced gamma-band activities (30–70 Hz) recorded by the sensors showing the SI and SII activities. (C) Topography of the induced gamma activities around the SI and SII areas.

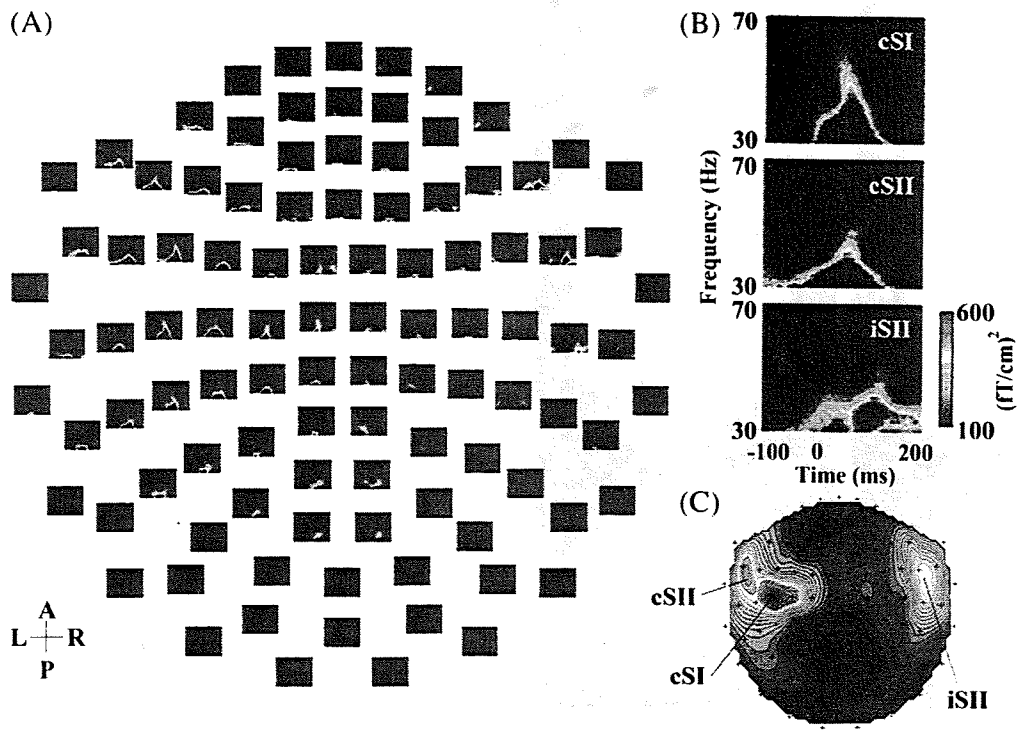

Fig. 6. (A) Temporal-frequency analysis for all gradiometer sensors in a representative MS patient. (B) Induced gamma activities recorded by the sensors showing the SI and SII activities. In contrast to normal subjects, the absolute power of the high-frequency gamma activities (50–70 Hz) is relatively reduced in cSI. (C) Topography of the induced gamma activities around the SI and SII areas.

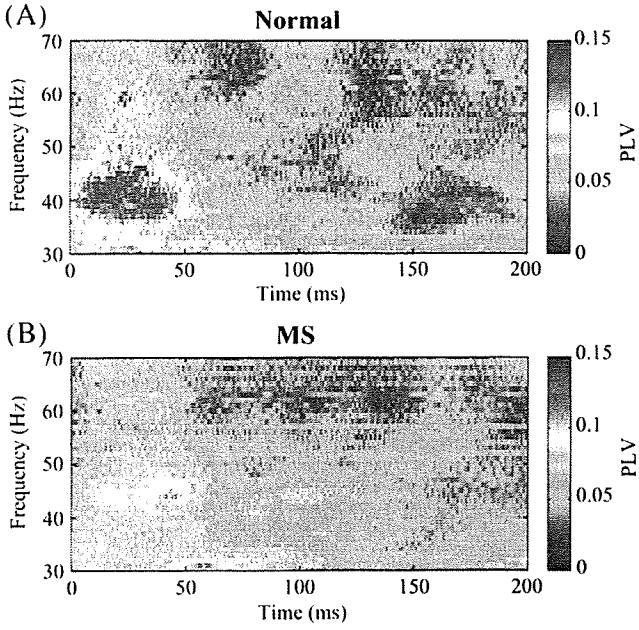

Fig. 7. Analysis of PLVs between cSI and cSII. (A) The grand average of PLVs in normal subjects shows increased PLVs in the entire gamma-frequency band (30–70 Hz). The high PLVs in the high-frequency gamma-band (50–70 Hz) are observed in the earlier latencies (mostly in the post-stimulus period of 20–50 ms), whereas those in the low-frequency gamma-band (30–40 Hz) last up to 100 ms. There are also some phase-locking activities of various frequencies during the later post-stimulus period (~100 ms). (B) In MS patients, decreased PLVs are noted in the entire frequency range.

of cSII started at around 20 ms after electrical stimulation of the median nerve, consistent with the latency of the direct thalamocortical conduction to SII. Likewise, short-latency responses in SII were reported by a study with direct cortical recording (Barba et al., 2002), which demonstrated that SEPs in SII could be generated at around 30 ms after the median nerve stimulation. Furthermore, transcranial magnetic stimulation delivered at the SII area at about 20 ms after electrical stimulation of the median nerve specifically caused facilitatory effect on motor reaction time (Raij et al., 2008), which proposed the presence of the direct thalamocortical pathway to SII. Although we could not record the early-latency evoked responses in SII, our results revealed a nonlinear relationship between the evoked responses in SI and SII. There was no significant correlation between the latencies of N20m and cSII both in normal subjects and MS patients. Moreover, analysis of SEFs showed no significant differences in the latencies and amplitudes of SII responses despite the prolonged latencies and decreased amplitudes of cSI deflections in MS patients. Thus, it is plausible that the early-latency gamma oscillations in SII, as reflected by the increased PLVs, might be partly mediated by the direct thalamocortical input to SII.

We demonstrated the decrease in PLVs between SI and SII in MS patients compared with normal control subjects. The temporal-frequency analysis demonstrated the preserved low-frequency gamma activities (30–40 Hz) in MS patients, whereas the phase synchronization was significantly impaired in the corresponding frequency range. We also found that the PLVs between cSI and cSII were reduced in the high-frequency gamma-band (50–70 Hz), while the power of the high-gamma activities was relatively decreased. One may argue that the decreased PLVs in the high-frequency gamma-band may be attributable to the reduced power of the activity in MS patients. However, PLV is theoretically independent of the power fluctuations (Lachaux et al., 1999). Because subcortical U-fiber lesions and periventricular white matter lesions in MS patients may frequently involve the intra- and interhemispheric associative pathways, the lesion load might significantly contribute to the decreased neuronal synchronization within the somatosensory cortical network. In accord with this view, the significance of such altered functional connectivity in MS patients was reported by some studies (Leocani et al., 2000; Cover et al., 2006; Arrondo et al., 2009), demonstrating disturbed neuronal synchrony in various frequency bands. The impaired interhemispheric functional connectivity in MS was also suggested by the non-correlation between the cSII and iSII latencies in the patient group. Although the assessment of intracortical connectivity within SI in MS patients has been performed by a recent MEG study using a synchronization index for the gamma-band activity (Tecchio et al., 2008), it is notable that this is the first MEG study to demonstrate impaired functional connectivity between SI and SII in MS.

Our study also raises a question regarding the general assumption that cSII and iSII are activated sequentially via the transcallosal fibers. We observed no significant difference in the latencies and amplitudes of iSII between the healthy subjects and MS patients, despite the altered cSI activity and the impairment of functional connectivity between cSII and iSII in the latter group. Our findings suggest that the functional disconnection of the bilateral somatosensory cortices does not have a significant impact on iSII activity. Similarly, a previous MEG study performed in patients with ischemic stroke lesions showed preserved responses of iSII, despite the diminished responses of cSI and cSII (Forss et al., 1999). These observations suggest that iSII receives direct input from the thalamus, and thus, the responsiveness of iSII is relatively independent of the activities of the contralateral somatosensory cortices.

The multifocality of the lesions in MS may be a methodological reservation of this study. The effect of individual lesions could not be simply weighed due to dissemination of the lesions in the CNS. In addition, we observed no significant changes in the evoked responses of SII despite the impaired SI response in MS. One may argue that thalamocortical inputs can be reduced both in SI and SII and that the SII activities could also be affected. Since our patients showed only mild disability, patients with more severe disability may reveal different characteristics on the SII responses. Alternatively, given that

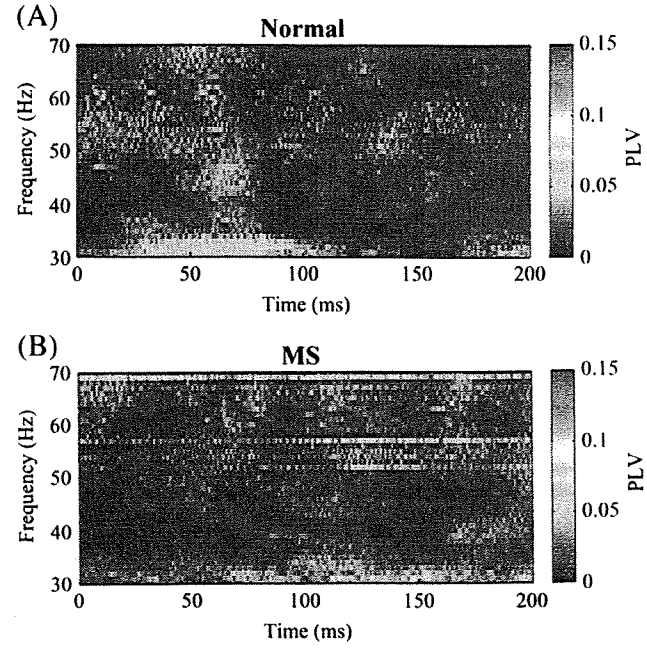

Fig. 8. Analysis of PLVs between cSII and iSII. (A) The grand average of PLVs in normal subjects shows significantly increased PLVs in the low-frequency gamma-band (30–40 Hz), which occurs between 30 and 100 ms. (B) Such an increase in PLVs is barely noticeable in MS patients.